

K-shell x-ray spectroscopy of atomic nitrogen

M. M. Sant'Anna* and A. S. Schlachter

*Advanced Light Source, Lawrence Berkeley National Laboratory,
University of California, Berkeley, California 94720, USA*

G. Öhrwall,[†] W. C. Stolte, and D. W. Lindle

Department of Chemistry, University of Nevada, Las Vegas, Nevada 89154-4003, USA

B. M. McLaughlin[‡]

*ITAMP, Harvard Smithsonian Center for Astrophysics, Mail Stop 14,
60 Garden Street, Cambridge, Massachusetts 2138, USA*

(Dated: October 26, 2018)

Absolute *K*-shell photoionization cross sections for atomic nitrogen have been obtained from both experiment and state-of-the-art theoretical techniques. Because of the difficulty of creating a target of neutral atomic nitrogen, no high-resolution *K*-edge spectroscopy measurements have been reported for this important atom. Interplay between theory and experiment enabled identification and characterization of the strong $1s \rightarrow np$ resonance features throughout the threshold region. An experimental value of 409.64 ± 0.02 eV was determined for the *K*-shell binding energy.

PACS numbers: PACS number(s): 32.80.Aa, 32.80.Ee, 32.80.Fb, 32.80.Zb

Keywords: photoabsorption, ions, synchrotron radiation, *K*-shell, x-ray

The atomic form of the seventh element, nitrogen, plays important roles in such diverse areas as x-ray astronomy, planetary physics, and materials science, fields that collectively span about 28 orders of magnitude on the length scale. Yet, to date, the *K*-shell spectroscopy of neutral atomic nitrogen has been the subject of limited theoretical predictions, untested by any high-quality experimental measurements. It is the purpose of this work to remedy this situation by reporting on high-resolution *K*-edge spectra, along with state-of-the-art theory, providing absolute atomic nitrogen *K*-shell cross sections for the first time.

In x-ray astronomy, the satellites *Chandra* and *XMM-Newton* are providing a wealth of x-ray spectra of astronomical objects. Spectroscopy in the soft-x-ray region (5-45 Å), including *K*-shell transitions of C, N, O, Ne, S, and Si and *L*-shell transitions of Fe and Ni, provides a valuable tool for probing extreme environments in active galactic nuclei, x-ray binary systems, cataclysmic variable stars, and Wolf-Rayet Stars [1, 2], as well as interstellar media (ISM) [3]. The latter, recent work, for example, demonstrated that x-ray spectra from *XMM-Newton* can be used to characterize ISM, provided accurate atomic oxygen *K*-edge cross sections are available. Analogous results concerning the chemical composition of ISM are expected with the availability of accurate atomic nitrogen *K*-edge cross sections [4].

In planetary science, inner-shell photoabsorption of atomic nitrogen is known to affect the energetics of the terrestrial upper atmosphere and, together with atomic oxygen and molecular nitrogen determine the ion-neutral chemistry and the temperature structure of the thermosphere through production of nitric oxide [5]. Since the nitric-oxide abundance is highly correlated with soft-x-ray irradiance, a full picture requires accurate knowledge of both the solar flux and the x-ray cross sections of these species. As demonstrated by observations using *Chandra*, atomic nitrogen and oxygen play a vital role in the terrestrial aurora, as well as similar phenomena on other planets, such as Jupiter [6].

In materials science, one application of *K*-edge spectroscopy of atomic nitrogen is in determining how the surface topology of a crystal affects dissociation of nitric oxide molecules adsorbed on stepped surfaces by measuring chemical shifts in the nitrogen *K* binding energies for different geometries [7, 8]. The structural sensitivity of such reactions is fundamental to the understanding of heterogeneous catalysis. Atomic *K*-edge spectroscopy may also prove critical to understanding a non-molecular phase of solid nitrogen, identified at high pressures via optical measurements, and likely related to an insulator-to-metal phase transition [9].

These diverse applications typically rely on tabulations of photoionization cross sections (*e.g.*, [10]) determined from a combination of basic theory and measurements of either molecular-phase or solid-phase N₂. A lack of high-quality data for atomic nitrogen has clearly impeded progress in some areas [11]. Unfortunately no experiments have been reported to date in the atomic nitrogen *K*-edge region. The primary barrier to such experiments, of course, is the difficulty of producing a dense atomic-nitrogen sample as a target. Experimental stud-

*Present address: Instituto de Física, Universidade Federal do Rio de Janeiro, Caixa Postal 68528, 21941-972 Rio de Janeiro RJ, Brazil

[†]Present address: MAX-Lab, Lund University, Box 118, Lund SE-221 00, Sweden

[‡]Present address: School of Mathematics & Physics, Queen's University of Belfast, Belfast BT7 1NN, UK

ies of atomic nitrogen in its ground state $1s^2 2s^2 2p^3 \ ^4S^{\circ}$ in the vicinity of the K edge may be further hampered by both the presence of metastable states of the atomic species as well as molecular resonances, such as $1s \rightarrow \pi^*$, in the N_2 gas used as a precursor in the production of atomic nitrogen.

In this Letter, we report high-resolution K -edge spectra of gas-phase atomic nitrogen, in combination with state-of-the-art theoretical calculations, in order to provide benchmark values for x-ray photoabsorption cross sections of this important species. The measurements were performed in the 390-418 eV photon-energy range, with a resolution of 60 meV, on the high-brightness undulator beamline 8.0 at the Advanced Light Source (ALS) synchrotron radiation facility in Berkeley, California. The atomic-nitrogen target was produced by partial dissociation of N_2 molecules in a microwave discharge [12] and introduced to the interaction region with the x-ray beam. Singly, doubly, and triply charged nitrogen cations were extracted from this region, selected with a magnetic mass analyzer [13], and their yields were measured as a function of photon energy. Careful extraction of the ion yields due to undissociated N_2 in the target permits determination of partial-ion yields due solely to photoionization of atomic nitrogen. Fortunately, while the intense $N_2 \ 1s \rightarrow \pi^*$ molecular resonance is present in this energy region, it does not overlap with any atomic-nitrogen features, allowing easy discernment of the nitrogen $1s 2s^2 2p^3 np$ core-excited atomic resonances.

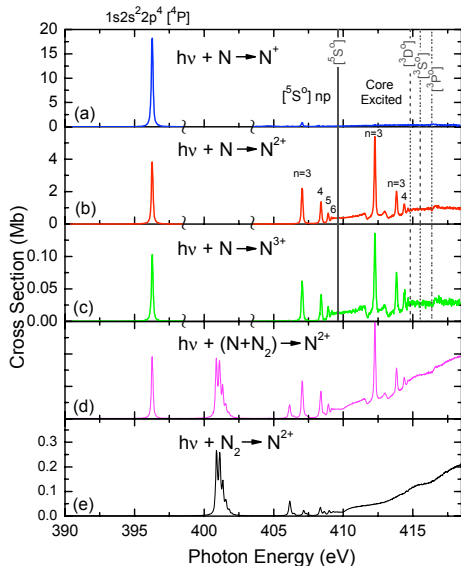


FIG. 1: Partial cross sections for photoionization of atomic nitrogen to (a) N^+ , (b) N^{2+} , and (c) N^{3+} . Figures (d) and (e) are experimental results from a mixture of atomic/molecular nitrogen and molecular nitrogen resulting in N^{2+} .

For the present measurements, gaseous N_2 was passed into a microwave cavity, and all products of the nitrogen plasma then flowed into the interaction region after passing through an L-shaped Pyrex tube [12].

It was found that collisions with the walls of this tube strongly quenched the nitrogen atoms created in long-lived metastable states ($1s^2 2s^2 2p^3 [^2D^{\circ}, ^2P^{\circ}]$) before they reached the interaction region, leaving only $1s^2 2s^2 2p^3 [^4S^{\circ}]$ ground-state atoms and molecular N_2 to interact with the x-rays (examples are shown in Fig 1(d) and 1(e)). To enhance the efficiency of the microwave discharge, a constant magnetic field, satisfying the electron-cyclotron resonance condition, was superimposed on the microwave cavity perpendicular to the 2.45 GHz electric and magnetic fields. The magnetic field aided in confinement and electron-cyclotron heating of the plasma, increasing the dissociation fraction of N_2 [14] (which is intrinsically low due to the strength of the triple bond), to 4% for the present experiments. While dissociation fractions as high as 80% for O_2 [12] and 20% for Cl_2 [15] have been achieved for other open-shell atoms, previous measurements of valence-shell photoionization of atomic nitrogen achieved only about 1% [16]. Thermal dissociation of N_2 , an alternate technique, is even less efficient [17].

The partial-ion yields measured as described above include contributions from both ground-state atomic nitrogen and molecular N_2 , but which differ as a function of photon energy. Since the spectroscopy of molecular N_2 is well known [18, 19], its presence provides an internal energy calibration. The cross section, $\sigma^{q+}(E)$, as a function of photon energy, E , for photoionization of atomic nitrogen to an ion of charge $+q$ can be obtained from [20]:

$$\sigma^{q+}(E) = C_{q+}(I_{\text{on}}^{q+} - f \times I_{\text{off}}^{q+}), \quad (1)$$

where I_{on}^{q+} , Fig 1(d), and I_{off}^{q+} , Fig 1(e), are normalized ion yields measured as a function of photon energy with the microwave discharge on or off, and C_{q+} is a constant dependent on the number density of nitrogen atoms and the ion-collection efficiency of the apparatus. Absolute data for single and multiple photoionization of N_2 [21] were used to determine values for the constants C_{q+} . The parameter $f = (n(N_2^{\text{on}})/n(N_2^{\text{off}}))$, with $n(N_2^{\text{on}})$ and $n(N_2^{\text{off}})$ being number densities of N_2 with the microwave discharge on or off, represents the fraction of N_2 molecules that do not dissociate in the discharge. The value of f is empirically chosen to eliminate the molecular peaks from the measured ion yields via a weighted subtraction [15, 16]. As noted above, the dissociation fraction, $1-f$, was about 4%. Finally, the collection efficiency for each ion N^{q+} produced by photoionization of atomic nitrogen was assumed equal to the collection efficiency of the same ion generated in dissociative photoionization of N_2 .

Figure 1 (a) – (c) shows partial cross section spectra for single, double, and triple photoionization of atomic nitrogen in the photon-energy range 390.0-418.5 eV. The energy region from 398.5-403.5 eV is intentionally left blank due to the presence of spurious structure from the subtraction of two large numbers in the vicinity of the $1s \rightarrow \pi^*$ molecular resonance. The strong peak in the cross section at 396.26 eV is due to $1s \rightarrow 2p$ promotion

from the $1s^2 2s^2 2p^3 [^4S^o]$ ground state to the lowest-lying core-excited $1s2s^2 2p^4 [^4P]$ autoionizing resonance state. At higher energies, the peaks correspond to transitions to $1s2s^2 2p^3 [^5S^o] np$ resonances below the lowest K -edge threshold as well as $1s2s^2 2p^3 [^3D^o] np$, $1s2s^2 2p^3 [^3S^o] np$, and $1s2s^2 2p^3 [^3P^o] np$ core-excited resonance states leading to higher-energy thresholds, as indicated in the figure and in Table I. Similar to molecular photofragmentation, N^+ is the prevalent ion formed, and most pronounced on the first resonance, whereas the other charge states are stronger for the higher lying resonances. Although atomic and molecular nitrogen have different electronic structures, our observed natural line width of 111 meV for the $1s2s^2 2p^4 [^4P]$ resonance is virtually identical to the 113 eV previously observed for the $N_2 (N 1s, \nu=0) \rightarrow (\pi_g^*, \nu')$ state [22].

State-of-the-art *ab-initio* theoretical methods are routinely used now [11, 23–30] to study inner-shell atomic processes, earlier studies were limited and primarily used the Hartree-Fock (HF) approximation [31–33]. The present theoretical predictions of atomic-nitrogen photoabsorption cross sections used the R-matrix method [34]: in this close-coupling approximation the core ion is represented by an N-electron system, and the total wavefunction expansion, $\Psi(E)$, of the $(N+1)$ -electron system for any symmetry $SL\pi$ is expressed as

$$\Psi(E) = A \sum_i \chi_i \theta_i + \sum_j c_j \Phi_j, \quad (2)$$

where χ_i is the core wavefunction in a specific state $S_i L_i \pi_i$ and θ_i is the wavefunction for the $(N+1)$ th electron in a channel labeled as $S_i L_i \pi_i k_i^2 l_i (SL\pi)$, with k_i^2 being its incident kinetic energy. The Φ_j are correlation wavefunctions of the $(N+1)$ -electron system that account for short-range correlation and orthogonality between continuum and bound orbitals, with c_j being the expansion coefficients. $\Psi(E)$ is a bound $(N+1)$ -electron wavefunction when the energy $E < 0$, with all channels closed, and a continuum wavefunction when $E > 0$, with some or all continuum channels open.

All of the (390) target levels in this work were represented by multi-configuration-interaction wavefunctions, obtained from $n = 2$ physical and pseudo $3\bar{l}$ orbitals of the residual N^+ ion core. The LS coupling R-matrix cross-section calculations included both radiative and Auger damping. The scattering wavefunctions were generated by allowing two-electron promotions out of the designated base configurations. The resonance features were resolved in the scattering problem with a fine-energy mesh of $1.36 \mu\text{eV}$ (10^{-7} Rydbergs).

Results for the autoionizing resonances are presented in Table I, indicating good agreement between experiment and theory. Precise energy calibration was achieved by comparing positions of the atomic-nitrogen features to resonances in the well-known molecular spectrum [18], specifically the narrow $3s\sigma$ (406.150 eV) and $3p\pi$ (407.115 eV) Rydberg transitions. The absolute energy scale was confirmed using the ν_0 vibrational level of the

$1s \rightarrow \pi^*$ resonance at 400.868 eV [18]. The atomic-nitrogen ion-yield spectra (Fig. 1) were fitted to Voigt functions for the peaks and arctangent functions for the thresholds to obtain accurate peak positions. Experimentally, the lowest-energy $1s \rightarrow np$ Rydberg series, with a $N^+ [^5S^o]$ core, was found to converge to a binding energy of 409.64 ± 0.02 eV, based on the Rydberg formula. This threshold is 0.30 ± 0.02 eV lower than the accepted value for the atomic nitrogen $1s$ binding energy in N_2 [18, 35].

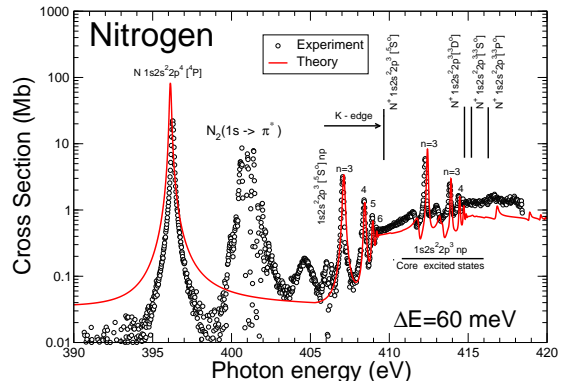


FIG. 2: Atomic-nitrogen total photoionization cross section. Theoretical results were convoluted with a 60 meV FWHM Gaussian to simulate experiment. Experimental results include molecular components between 400 and 406 eV.

The experimental cross sections for photoionization of atomic nitrogen to N^+ , N^{2+} , and N^{3+} ions in Fig. 1 were summed to obtain the total photoionization cross section, shown in Fig. 2 along with theoretical predictions using the R-matrix method. Good agreement is found between theory and experiment for both the resonance energies and absolute cross sections. Observed differences in the background between experiment and theory are consistent with uncertainties resulting from the experimental normalization procedure. Approximately 96% of our partially dissociated target is composed of N_2 and as we are subtracting in (1) two large numbers of comparable magnitude, the contribution from N_2 in I_{on}^{q+} is not completely equivalent to the room-temperature I_{off}^{q+} , the vibrational structure is different. This is clearly observed in Fig. 2 by the remaining π^* resonance with the discrepancy manifesting itself more with increasing photon energy. Our results demonstrate strong resonant features dominate the photoionization cross section of atomic nitrogen in the vicinity of the K edge, the atomic resonances differing significantly from those in molecular nitrogen which are absent in existing tabulations. Rydberg states above the first ionization threshold at 409.64 eV show clear Fano-Beutler profiles, indicating strong interferences between the core-excited intermediate resonance states and the open continua.

The experiments were supported by NSF, DOE, the DOE Facilities Initiative, Nevada DOE EPSCoR, and CNPq (Brazil). The theoretical work was supported

TABLE I: Atomic nitrogen $1s2s^22p^3 np \ ^4P$ core-excited autoionizing resonances converging to the $^5S^\circ$, $^3D^\circ$, $^3S^\circ$ and $^3P^\circ$ series limits. Results are given for the resonance positions (eV), natural linewidths Γ at FWHM (meV) and quantum defects μ . Experimental linewidths were extracted from the ion-yield measurements in Fig. 1 by fitting Voigt profiles to the peaks assuming a Gaussian instrumental contribution of 60 meV for each peak.

Resonances	Energy (Expt)	Energy (Theory)	Γ (Expt)	Γ (Theory)	μ (Expt)	μ (Theory)
$1s2s^22p^4$	396.27 ± 0.02	396.18	111 ± 10	109	0.99 ± 0.02	0.99
$1s2s^22p^3[^5S^\circ]3p$	407.05 ± 0.02	407.08	99 ± 20	107	0.71 ± 0.02	0.70
$1s2s^22p^3[^5S^\circ]4p$	408.40 ± 0.02	408.46	89 ± 20	106	0.69 ± 0.02	0.61
$1s2s^22p^3[^5S^\circ]5p$	408.92 ± 0.03	408.94	95 ± 10	98	0.65 ± 0.03	0.59
$1s2s^22p^3[^5S^\circ]6p$	409.16 ± 0.04	409.18	80 ± 10	80	0.68 ± 0.04	0.56
$^5S^\circ$ series limit	409.64 ± 0.02	—	—	—	—	—
—	—	—	—	—	—	—
$1s2s^22p^3[^3D^\circ]3p$	412.28 ± 0.02	412.42	83 ± 10	80	0.69 ± 0.02	0.62
$^3D^\circ$ series limit	414.82 ± 0.05	—	—	—	—	—
—	—	—	—	—	—	—
$1s2s^22p^3[^3S^\circ]3p$	412.96 ± 0.06	413.14	237 ± 20	235	0.70 ± 0.06	0.62
$1s2s^22p^3[^3S^\circ]4p$	414.38 ± 0.03	414.45	116 ± 10	107	0.56 ± 0.03	0.45
$^3S^\circ$ series limit	415.53 ± 0.05	—	—	—	—	—
—	—	—	—	—	—	—
$1s2s^22p^3[^3P^\circ]3p$	413.83 ± 0.02	413.91	100 ± 10	108	0.68 ± 0.02	0.64
$^3P^\circ$ series limit	416.36 ± 0.05	—	—	—	—	—

by NSF and NASA grants to ITAMP at the Harvard-Smithsonian Center for Astrophysics and the Smithsonian Astrophysical Observatory. The computational work was done at the National Energy Research Scien-

tific Computing Center in Oakland, CA and on the Tera-grid at the National Institute for Computational Sciences (NICS), in Knoxville, TN, which is supported in part by NSF.

-
- [1] S. L. Skinner *et al.*, *Astronom. J.* **139**, 825 (2010).
[2] R. Ignace *et al.*, *Astron. and Astrophys.* **408**, 353 (2003).
[3] J. García *et al.*, *Astrophys. J.* **731**, L15 (2011).
[4] J. García, *private communication*.
[5] R. Link, *private communication*.
[6] A. Bhardwaj *et al.*, *J. Atm. Solar-Terr. Phys.* **69**, 179 (2007).
[7] J. Rempel *et al.*, *J. Phys. Chem. C* **113**, 20623 (2009).
[8] F. Esch *et al.*, *J. Chem. Phys.* **110**, 4013 (1999).
[9] A. F. Goncharov *et al.*, *Phys. Rev. Lett.* **85**, 1262 (2000).
[10] B. L. Henke *et al.*, *At. Data Nucl. Data Tables* **54**, 181 (1993).
[11] B. M. McLaughlin, *Spectroscopic Challenges of Photoionized Plasma (ASP Conf. Series vol 247)* ed G. Ferland and D. W. Savin (San Francisco, CA: Astronomical Society of the Pacific) p 87, (2001)
[12] W. C. Stolte *et al.*, *J. Phys. B* **30**, 4489 (1997).
[13] W. C. Stolte *et al.*, *J. Phys. B* **41**, 145102 (2008).
[14] J. Geddes *et al.*, *Plasma Sources Sci. Technol.* **3**, 58 (1994).
[15] J. A. R. Samson, *et al.*, *Phys. Rev. Lett.* **56**, 2020 (1986).
[16] J. A. R. Samson and G. C. Angel, *Phys. Rev. A* **42**, 1307 (1990).
[17] M. M. Sant’Anna *et al.*, *Nucl. Instrum. Methods Phys. Res. B* **132**, 306 (1997).
[18] C. T. Chen *et al.*, *Phys. Rev. A* **40**, 6737 (1989).
[19] S. K. Semenov *et al.*, *J. Phys. B* **39**, 375 (2006).
[20] J. A. R. Samson and P. N. Pareek, *Phys. Rev. A* **31**, 1470 (1985).
[21] W. C. Stolte *et al.*, *At. Data Nucl. Data Tables* **69**, 171 (1998).
[22] M. Kato *et al.*, *J. Electron. Spectrosc. and Relat. Phenom.* **160** 39, (2007).
[23] A. S. Schlachter *et al.*, *J. Phys. B* **37**, L103 (2004).
[24] S. W. J. Scully *et al.*, *J. Phys. B* **38**, 1967 (2005).
[25] J. García *et al.*, *Astrophys. J. Suppl. Ser.* **158**, 68 (2005).
[26] S. W. J. Scully *et al.*, *J. Phys. B* **39**, 3957 (2006).
[27] A. Müller *et al.*, *J. Phys. B* **42**, 235602 (2009).
[28] J. García *et al.*, *Astrophys. J. Suppl. Ser.* **185**, 477 (2009).
[29] A. Müller *et al.*, *J. Phys. B* **43**, 135602 (2010).
[30] M. F. Hasoğlu *et al.*, *Astrophys. J.* **724**, 1296 (2010).
[31] R. F. Reilman and S. T. Manson, *Astrophys. J. Suppl. Ser.* **40**, 815 (1979).
[32] J. Yeh, *Atomic Calculation of Photoionization Cross-Sections and Asymmetry Parameters*, Gordon & Breach, New York, USA (1993).
[33] C. T. Chantler, *J. Phys. Chem. Ref. Data* **24** 71 (1995).
[34] P. G. Burke and K. A. Berrington, *Atomic and Molecular Processes: an R-matrix Approach*, IOP Publishing, Bristol, UK (1993).
[35] G. Johansson *et al.*, *J. Electron. Spectrosc. and Relat. Phenom.* **2** 295, (1973).